Prediction of Polymer Flood Performance

J. T. PATTON

K. H. COATS
MEMBERS AIME

G. T. COLEGROVE

COMPUTER/BIOENGINEERING INSTITUTE, INC.
HOUSTON, TEX.
INTERNATIONAL COMPUTER APPLICATIONS LTD.
HOUSTON, TEX.
KELCO CO.
HOUSTON, TEX.

ABSTRACT

This experimental and numerical study was performed to estimate the incremental oil recovery by pattern polymer flooding in a California viscous-oil reservoir. Results indicate that adding 270-ppm Kelzan to the normal flood water will boost oil production by 42 percent (at 1 PV injected) and will reduce water handling costs sharply. This corresponds to $8.35 incremental oil/$1.00 polymer injected, taking into account the 30 percent pore volume bank of polymer solution. The 28.6 percent additional oil recovery predicted at 0.5 PV injected yields a return of $4.60 incremental oil/$1.00 polymer injected.

The field predictions are based on (a) laboratory measurements of polymer solution viscosity, adsorption and dispersion upon displacement by normal water in a sand representative of the reservoir, (b) linear laboratory oil displacement experiments using brine and polymer solution, and (c) a numerical model developed to simulate linear or five-spot polymer floods in single-layer or stratified reservoirs.

The paper presents an analytical solution to the linear polymer flood problem, which provides a check on accuracy of the numerical model and a quick estimate of additional oil recovery by line-drive polymer floods. The numerical model developed indicates that additional oil recovery by polymer flooding is sensitive to polymer bank size and adsorption level and is insensitive to the extent of dispersion active at the trailing edge of the polymer slug.

INTRODUCTION

The benefits of improving the mobility ratio, λ_o/λ_w, on waterflood performance is well documented[1-8] and research on how best to effect this improvement has been considerable. Both producers and chemical manufacturers, spurred on by the vast reserves of oil which will be otherwise abandoned, have sought to resolve the problem. Currently, two types of additives are being marketed and field tested with promising results. Both additives increase oil recovery by lowering the mobility of the flood water, λ_w. However, they effect this lowering by distinctly different mechanisms.

Mobility of the flood water is given by:

$$\lambda_W = k_W/\mu_W \cdot$$

Hence, one may elect to either increase viscosity, μ_w, or decrease effective permeability, k_w. Viscosity can be increased by adding small amounts of a water-soluble polymer. To be effective at the flood front this additive should exhibit minimum adsorption on the pore surfaces.

Polymers showing minimal adsorption are generally a combination nonionic-anionic type. The negative charge repels the clay platelets to reduce adsorption and the nonionic portion provides the brine tolerance required for reservoir applications. A polymer of this type, Kelzan M, was chosen for the study. The alternate method of lowering mobility is equally well known.[5] It consists of adding to the flood water a polymer designed to adsorb on the pore surfaces, thereby physically reducing the available flow area.

This study was performed to estimate the additional oil recovery by pattern polymer flooding using Kelzan in a California viscous-oil reservoir. Laboratory experiments were performed to estimate polymer solution viscosity, adsorption and dispersion upon displacement by normal injection water. Waterflood and polymer flood oil recovery curves were obtained for a laboratory core packed with sand representative of the reservoir. A numerical model was developed to simulate polymer floods in linear or five-spot patterns in single-layer or stratified reservoirs. An analytical solution to the linear polymer flood problem was developed to provide a quick estimate of incremental oil obtainable by polymer flooding and to provide a check on the accuracy of the numerical model.

Subsequent sections in this paper describe the analytical solution, the numerical model, the laboratory experiments and, finally, the predicted incremental oil recoveries obtainable by polymer slug injection into the reservoir.

ANALYTICAL CALCULATION OF LINEAR POLYMER FLOODS

The mathematical model for a linear polymer flood consists of two equations expressing conservation of mass of water and polymer:

$$- u\frac{\partial f}{\partial x} = \phi\frac{\partial S}{\partial t} \qquad \ldots \ldots \ldots \text{(1a)}$$

$$- u\frac{\partial (fC)}{\partial x} = \phi[\frac{\partial (SC)}{\partial t} + \frac{\partial C_s}{\partial t}] \quad , \quad \text{(1b)}$$

where u = volumetric total velocity, cu ft/sq ft-D

f = fractional flow of water, $\lambda_w/(\lambda_w + \lambda_o)$

λ_w = water mobility, k_{rw}/μ_w

S = water saturation

C = polymer concentration, gm/cc

C_s = adsorbed polymer concentration, gm/cc of pore space

Fractional flow f is a function of saturation and concentration. Assumptions inherent in Eqs. 1a and 1b or in their subsequent analytical solution are:

A. Dispersion of the concentration profile is negligible.

B. Fluid and rock compressibilities may be neglected.

C. The flood is isothermal.

D. Adsorption is effectively instantaneous at oil displacement rates encountered in the reservoir.

E. Connate water is completely displaced, with minimal or no mixing by the injected polymer water.

F. Water viscosity is a function of concentration only. If it is dependent upon shear, then the variation of shear rate through the linear system is assumed negligible.

G. The adsorption isotherm is of negative curvature as shown in Fig. 1.
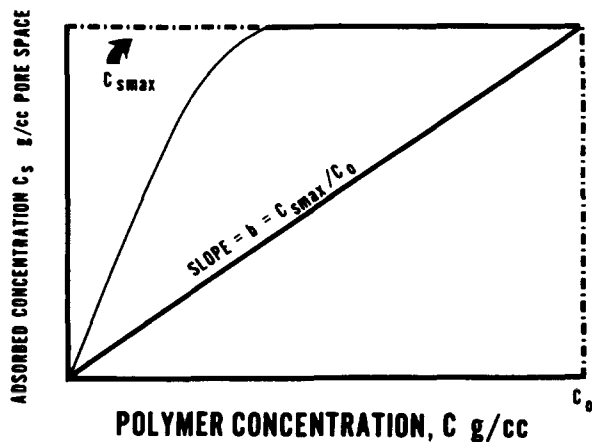

FIG. 1 — POLYMER ADSORPTION ISOTHERM.

H. Effects caused by oil-water capillary pressure are negligible.

Assumption E is based in part on the work of Brown,[9] whose experiments showed a strong tendency toward piston displacement of connate water by injected water in a normal water flood. Mungan et al.[6] observed in laboratory flow tests the formation of a connate water bank ahead of the polymer front. However, Jones[7] observed in a field pilot test the presence of polymer in the first water produced, thus indicating no connate water bank formation ahead of the polymer front.

For the above assumptions and the case of continuous polymer water injection, Eqs. 1a and 1b can be solved analytically using the method of characteristics and shock discontinuity theory. This analytical solution is illustrated here in the context of examples. Fig. 2 shows laboratory measured water-oil relative permeability curves for a 6,000-md unconsolidated, Nevada sand representative of a California viscous-oil reservoir. Fig. 3 shows the water fractional flow curves for the cases of normal water, $\mu_w = 1$ cp, and polymer
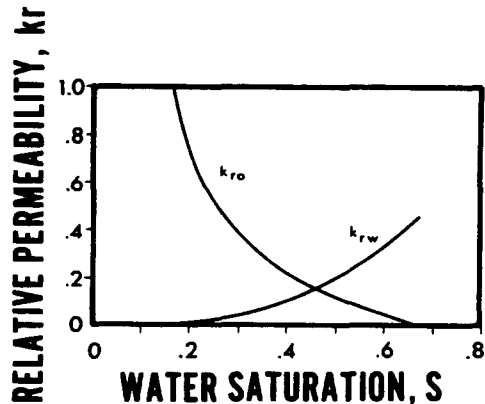

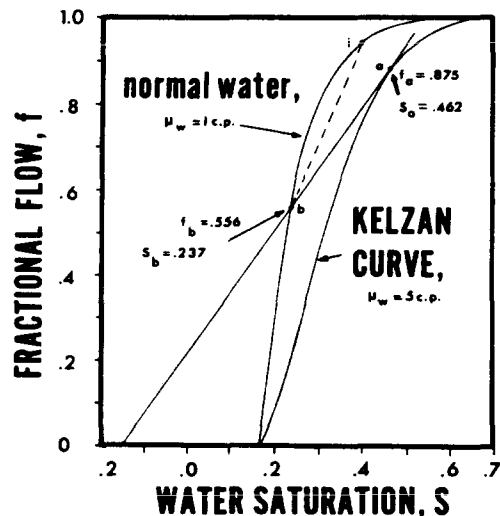FIG. 2 — RELATIVE PERMEABILITY CURVES, 6,000-MD SAND.

FIG. 3 — FRACTIONAL FLOW CURVES WITH AND WITHOUT POLYMER.

water with an apparent or effective μ_w = 5 cp. Oil viscosity is 34 cp and connate water saturation is 0.168.

We will first illustrate the solution for the case of an initial connate water saturation in the linear sand. Fig. 4 shows the water saturation and polymer concentration profiles after injection of 0.1 PV of polymer water. The saturation profile exhibits two discontinuities at x_{D1} and x_{D2} as noted on Fig. 4. The discontinuity x_{D1} travels at a rate

$$\frac{dx_{D1}}{dI} = \frac{f_a}{S_a + b} , \quad . . . . \quad (2)$$

where $x_D = x/L$

L = length of the linear sand

I = pore volumes water injected, $qt/L\phi$

$b = C_{smax}/C_0$ (Fig. 1)

C_0 = polymer feed concentration

The values of f_a, S_a correspond to Point a on the polymer water fractional flow curve shown in Fig. 3 and are determined by drawing a tangent to that fractional flow curve from a point located b units to the left of the origin on the water-saturation axis. An adsorption level of b = 0.15 was used in the tangent construction shown.

The polymer water concentration profile is sharp as shown on Fig. 4, and its leading edge travels at the rate given in Eq. 2.

A connate water bank forms ahead of the polymer water and the "strength" S_b of this bank is given by the intersection of the above described tangent with the normal water fractional flow curve (Fig. 3). This connate water bank front travels with velocity

$$\frac{dx_{D2}}{dI} = \frac{f_b - f_i}{S_b - S_i} = \frac{f_b}{S_b - S_i} . \quad . (3)$$

Actually the existence of this discontinuity at x_{D2} depends upon positive curvature of the normal water fractional flow curve between S_i and $S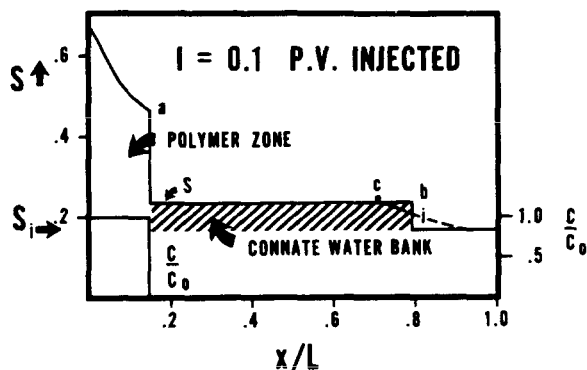_b$. If this curvature is negative, then lower saturations in this region travel faster than higher saturations and the shape of the connate water bank front is as shown by the dashed line on Fig. 4. The distinction between these two cases is largely immaterial since Point c on the saturation profile travels with velocity $dx_{Dc}/dI = (df/dS)_{S=S_b}$, and this is a large velocity resulting in very early breakthrough of saturation S_b.

Water saturations greater than S_a travel with velocities given by

$$\frac{dx_D}{dI}\Big)_S = \frac{df}{dS}\Big)_S , \quad . . . . \quad (4)$$

where the derivatives df/dS are taken from the polymer water fractional flow curve. Eqs. 2 through 4 completely characterize the analytical water saturation profile while Eq. 2 gives the position of the polymer concentration profile front.

In accordance with Eqs. 2 and 3, the connate water bank will break through at $I = (S_b - S_i)/f_b$, and the polymer front and associated saturation discontinuity will break through at $I = (S_a + b)/f_a$. Fig. 5 shows the oil recovery curve constructed from Eqs. 2 through 4 and, for comparison, the recovery curve for a normal waterflood as calculated by the Buckley-Leverett method.[10]

Fig. 6 shows the analytical saturation and concentration profiles at 0.39 PV water injected for a case where mobile water is initially present. Initial water saturation is 0.4, indicated by Point i on Fig. 3. For this illustration, the adsorption factor b is 0.3. The frontal saturation S_a (see Fig. 6) is determined by drawing a tangent to the polymer water fractional flow curve on Fig. 3 from a point on the saturation axis located at $S = -0.3$. The point of tangency is at $S_a = 0.478$, $f_a = 0.892$. The intersection of this tangent with the normal water fractional flow curve gives the "strength" of the oil bank formed ahead of the polymer front, i.e., $S_b = 0.251$ and $f_b = 0.634$.

The sharp polymer front and the associated saturation discontinuity ab travel at the velocity

FIG. 4 — ANALYTICAL WATER SATURATION AND POLYMER CONCENTRATION PROFILES FOR LINEAR POLYMER FLOOD.
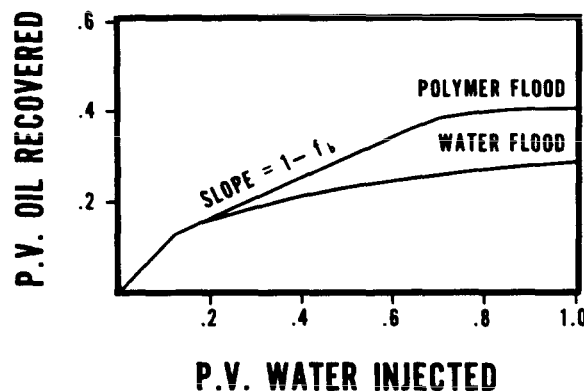

FIG. 5 — ANALYTICAL OIL RECOVERY CURVES FOR LINEAR WATER AND POLYMER FLOODS.

$$\frac{dx_{D1}}{dI} = \frac{f_a - f_b}{S_a - S_b} = \frac{f_a}{S_a + b} \quad \ldots \ldots (5)$$

This saturation discontinuity will break through at $x = L$ after injecting $I = (S_a + b)/f_a$ pore volumes of water. The leading edge of the oil bank, ic, travels at the rate

$$\frac{dx_{D2}}{dI} = \frac{f_i - f_b}{S_i - S_b}$$

and will break through after injecting $(S_i - S_b)/(f_i - f_b)$ pore volumes.

Fig. 7 shows the analytically calculated oil recovery curve for the polymer flood and, for comparison, the recovery curve for a normal waterflood. The abrupt change in slope of the oil recovery curve reflects the breakthrough of the oil bank.

This analytical method of calculation is a quick and easy procedure to estimate the additional oil recoverable by a linear polymer flood as a function of oil viscosity, effective polymer water viscosity and level of adsorption.

NUMERICAL SIMULATION OF FIVE-SPOT POLYMER FLOODS

The numerical model described here simulates linear or five-spot polymer floods in a single-sand reservoir or in a stratified reservoir consisting of several noncommunicating sands of varying thickness, permeability and porosity. Different relative permeability curves and initial water and gas saturations may be used for each different sand layer in the stratified case.

The model utilizes the "streamtube" approach introduced by Higgins and Leighton.[11] Each sand layer of the reservoir is divided into a number of tubes connecting the injector to the producer in 1/8 of a fi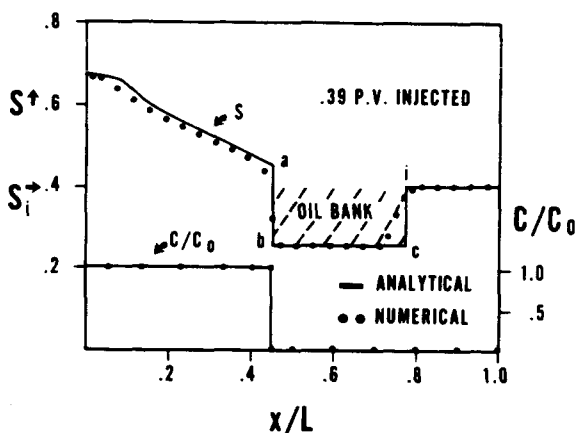ve-spot. Each tube is divided into a number of equal-volume increments, and Eqs. 1a and 1b are solved numerically for each tube. The total injection rate is allocated among the tubes each time step in accordance with the current conductances of the tubes. These conductances vary from time step to time step because of the different rates of displacement among the tubes. The model calculates and prints each time step the injectivity in BPD/psi pressure difference between injector and producer. Polymer water viscosity is represented in the model as a function of concentration and shear rate.

The model has been programmed in FORTRAN IV and requires about 20 seconds of UNIVAC 1108 time for 1 PV injected into a single-layer five-spot divided into eight tubes (1/8 of a five-spot) and 30 increments per tube. Details of the model are given in the Appendix. Here we simply describe it in general and give some comparisons with analytical solutions and experimental data to indicate the model's validity.

The model allows specification of an arbitrary polymer bank size and accounts for dispersion at the trailing edge of the bank. Polymer adsorption is assumed irreversible so that the leading edge of the bank advances at a lower rate than the trailing edge. This results eventually in a "breakdown" or disappearance of the polymer bank. Dispersion hastens this breakdown although it really just smears the (feed) bank concentration at lower levels over the distance traveled by the bank.

Several checks have been performed to test the model's validity. First, the model was run with initial water saturation of 100 percent to check its calculation of injectivity index. Muskat[12] gives the five-spot formula.

$$q = \pi k h \Delta p / [\mu (\ln \frac{d}{r_w} - .619)] \quad ,(6)$$

where q = injection rate, cu ft/D

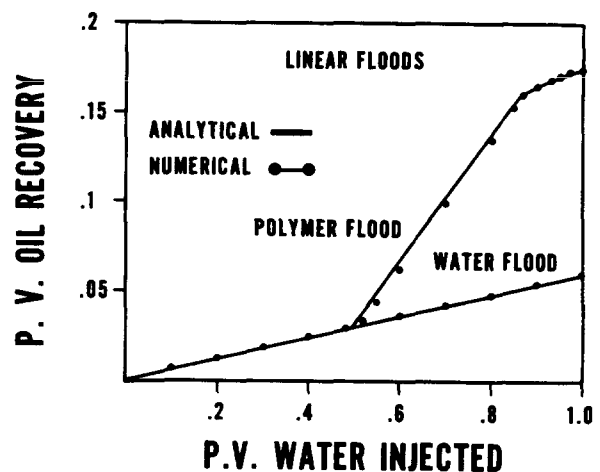k = md × 0.00633

h = sand thickness, ft

FIG. 6 — COMPARISON OF ANALYTICAL AND NUMERICAL SATURATION AND CONCENTRATION PROFILES FOR LINEAR POLYMER FLOOD.

FIG. 7 — ANALYTICAL AND NUMERICAL OIL RECOVERY CURVES.

Δp = pressure drop from injector to producer, psi

μ = fluid viscosity, cp

d = distance from injector to nearest producer, ft

r_w = wellbore radius, ft

The resistances of the tubes in the model are calculated accounting for the varying tube cross-sectional area from well to well. This calculation results in exact agreement between model injectivity (for the single-fluid case) and that given by Eq. 6.

Since the model can be run for an arbitrary number of tubes and layers, it was run for a single tube to compare results with the analytical linear polymer flood calculation. Fig. 6 compares the numerical results from the model with the analytical solution. Fig. 7 compares the numerically calculated oil recovery curves (for water and polymer floods) with the analytical ones. These figures show that the individual tube numerical calculation is quite accurate.

The model was run for a single-layer five-spot with normal water injection to simulate the laboratory five-spot floods performed by Douglas et

al.[13] These four laboratory waterfloods were performed for oil-water viscosity ratios varying from 0.083 to 754 — a range of nearly 10,000 in mobility ratio. Fig. 8 compares the laboratory oil recovery curves with those calculated by the numerical model.

Figs. 9 and 10 show the effects of adsorption and dispersion on the calculated polymer bank shape and breakdown. The linear flood results shown were calculated by the numerical model using the relative permeability curves of Fig. 2, a polymer bank size of 0.2 PV, oil viscosity of 34 cp, and an adsorption level corresponding to b = 0.3. Polymer water viscosity was represented as a linear function of concentration, $\mu_w = 1 + 4C/C_0$. For the case of zero dispersion, Fig. 9 shows that the polymer bank maintains its full feed concentration until the sharp trailing edge catches up to the leading edge, at which instant the bank disappears. Fig. 10 shows that dispersion causes a smearing of the trailing edge resulting in a more gradual breakdown of the polymer bank.

The effect of this trailing-edge dispersion on the oil recovery curve for the linear flood is very little — cumulative oil recoveries for the two runs at 0.6 PV injected were 0.296 for zero dispersion and 0.291 for dispersion = 0.3.* The effect of trailing-edge dispersion on the calculated oil recovery for a five-spot flood is equally negligible. Fig. 11 shows

*This dispersion factor (0.3) is related to the normal dispersion coefficient D as described in the Appendix.
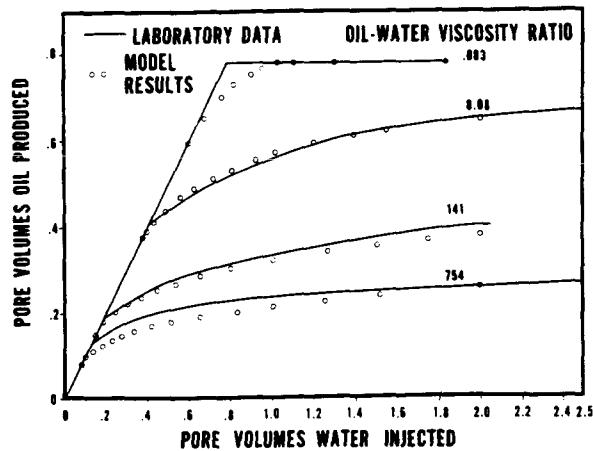
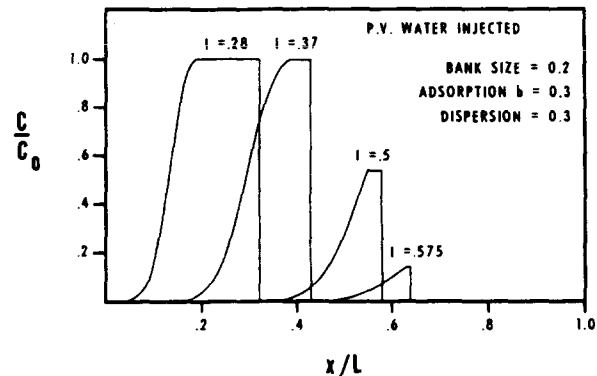FIG. 8 — COMPARISON OF NUMERICAL MODEL RESULTS WITH LABORATORY FIVE-SPOT WATER-FLOOD DATA.[5]
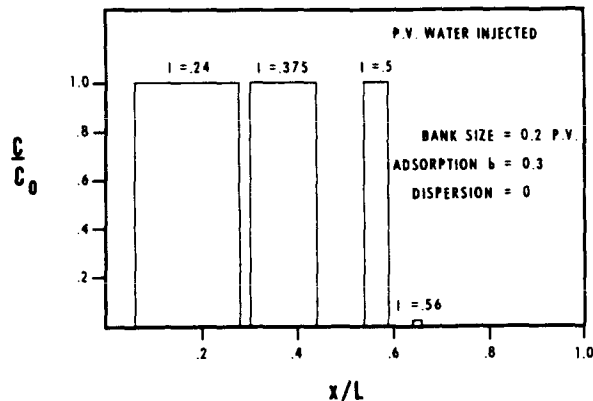
FIG. 10 — EFFECT OF DISPERSION ON POLYMER SLUG PROFILE.
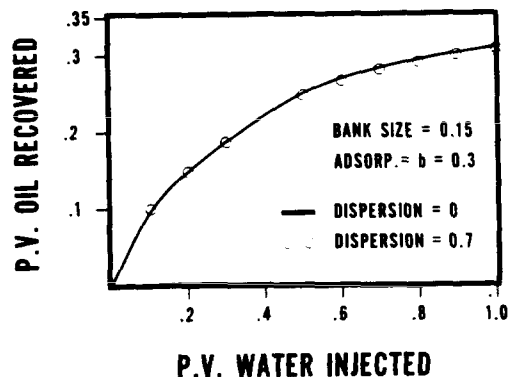
FIG. 9 — ADSORPTION CAUSES POLYMER BANK BREAKDOWN.

FIG. 11—EFFECT OF DISPERSION ON CALCULATED FIVE-SPOT OIL RECOVERY CURVE.

calculated oil recovery for a five-spot using a 15 percent PV polymer bank and an adsorption level of $b = 0.3$. Calculated oil recovery at 1 PV injected was 0.31 PV for zero dispersion and 0.307 PV for dispersion = 0.7.

In these and other test runs, significant trailing-edge dispersion was achieved in that concentration and was smeared over many grid blocks behind the leading edge of the slug. In no case was this dispersion found to significantly affect the oil recovery curve. However, it should be noted that polymer water viscosity was treated as a linear function of concentration. Thus, qualitatively speaking, the insensitivity of results to the dispersion might reflect in part, the fact that half the concentration smeared over twice the distance ℓ will have about the same effect as full concentration over distance ℓ.

EXPERIMENTAL TESTS AND RESULTS

POLYMER VISCOSITY

Fig. 12 shows the effects of Kelzan M concentration and shear-rate on polymer water viscosity. The effect of shear rate was determined by varying spindle speed on an LVT Brookfield viscosimeter with the U.L. attachment. The decrease in viscosity at high shear rates is desirable from an injectivity standpoint. It is conceivable that polymers having strong friction reducing properties might show higher injectivities than water alone.

POLYMER ADSORPTION

A general criticism directed at mobility control agents has been their adsorption on reservoir rock.[6] Data on a few specific types, misapplied to polymers in general, has resulted in some confusion. Polymers do adsorb, but the quantity varies widely from one polymer to another. It is, therefore, necessary to quantify adsorption for a specific polymer before its flow behavior can be accurately predicted.
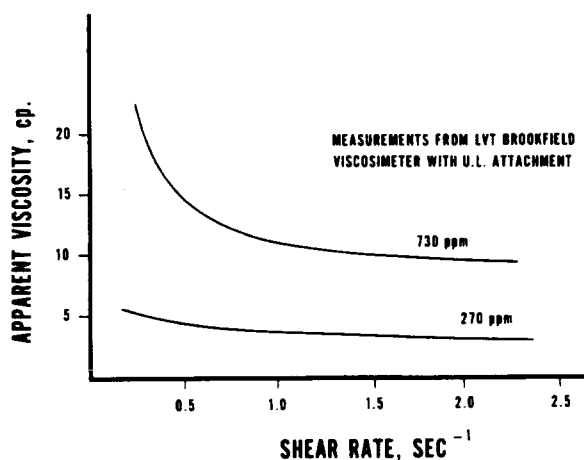
A good technique for quantifying adsorption is to flow the polymer solution through a brine-saturated tube packed with a known amount of fresh adsorbent, in this case reservoir sand. In the absence of adsorption and dispersion, the effluent concentration will rise from zero to feed concentration at 1 PV injected. Dispersion results in an earlier breakthrough and a gradual rise from zero to feed concentration after 1 PV injected. The $0.5C_0$ concentration will appear roughly at 1 PV injected. Adsorption will shift the effluent profile to the right and the $0.5C_0$ concentration will appear roughly at $1 + b$ PV injected.

Such a test was performed with a solution of Kelzan M at the concentration which was used in the subsequent oil displacement experiments. The sand pack employed was a 24- × 5-in. glass tube packed with Simplots 135 Nevada sand. The resulting effluent concentration curve shown in Fig. 13 indicates an adsorption factor b of about 0.15. The specific adsorption of Kelzan M on the Nevada sand is 0.0025 lb/cu ft PV.

The strong asymmetry in the effluent curve indicates that a secondary factor, other than adsorption, tends to remove polymer from solution. This secondary effect could result from any one or a combination of: (A) the filtration or mechanical entrapment discussed by Gogarty,[3] whereby polymer clumps or aggregates are trapped by the smaller pore restrictions in the model; (B) noninstantaneous adsorption onto the sand; (C) noninstantaneous diffusion of polymer into dead-end or relatively stagnant pore space pockets. The most plausible of those is Effect A.

TRAILING-EDGE DISPERSION

It is usually desirable to propel an injected polymer bank with normal injection water. The less viscous injection water naturally tends to finger into the polymer slug and smear the trailing edge of the polymer band.

Data on dispersion of the 270-ppm Kelzan M solution were obtained in a 1- × 48-in. cylindrical model similar to the one used for adsorption and oil displacement studies. The added length served to improve the accuracy of the data shown in Fig. 14. The dashed curve shows how the breakout curve

FIG. 12 — EFFECTS OF SHEAR RATE AND CONCENTRATION ON VISCOSITY OF KELZAN M POLYMER WATER.
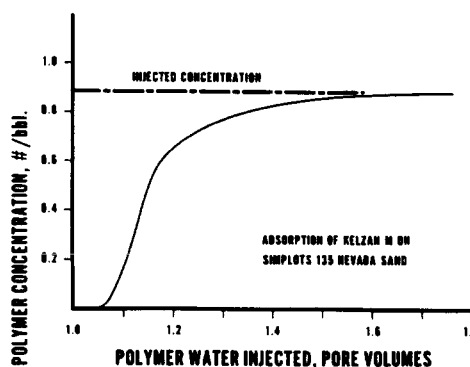

FIG. 13—BREAKOUT CURVE QUANTIFIES POLYMER ADSORPTION.

would appear with no dispersion. The skewed curve actually obtained indicates the large influence dispersion can have in laboratory core tests. The early breakthrough and exaggerated tailing out of the back edge of the polymer solution indicates that the sand pack may contain pores which are by-passed when filled or blocked by polymer water. This tailing was also observed and reported by Gogarty.[3]

Three experimental runs with superficial velocities ranging from 10 to 30 ft/D all gave essentially the same effluent concentration curve shown in Fig. 14. This insensitivity to rate is a characteristic of the normal dispersion or axial mixing model employed to represent mixing in miscible displacements. This dispersing model includes a dispersion coefficient D (area/time) which is linearly proportional to velocity at velocities sufficiently larger than those where molecular diffusion dominates.[14] The difference ΔI between $I_{0.9}$ and $I_{0.1}$ (i.e., pore volumes injected when the 0.9 and 0.1 C/C_0 concentrations, respectively, appear in the effluent) for this dispersion model is inversely proportional to the square root of the distance traveled, L, by the mean concentration $0.5\,C/C_0$. A rough scaling of the effluent concentration profile shown in Fig. 14 to a field length of 1,000 ft then gives

$$\Delta I_{field} = (1.65 - .52)\sqrt{\frac{4}{1,000}}$$

$$= .0715 \qquad \cdot \ \cdot \ \cdot \ \cdot \ \cdot \ \cdot \ (7)$$

This estimate indicates that dispersion of the trailing edge may be considerably less significant in a field flood than in a laboratory flood.

We emphasize that this field-scale dispersion level is a rough estimate based on an assumed applicability of the usual dispersion model (D proportional to velocity). No evidence is available or presented here to prove that the trailing edge mixing caused by the adverse water-polymer water viscosity ratio is actually described by this dispersion model.
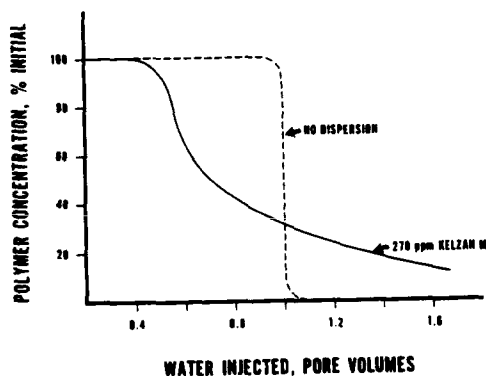
OIL DISPLACEMENT EXPERIMENTS

A 36- × 1½-in. cylindrical tube was packed with 6,000-md Nevada sand, saturated with brine and driven to connate water saturation of 16.8 percent by 34 cp oil. Subsequent brine injection resulted in the (normal waterflood) oil recovery curve shown in Fig. 15. Two polymer floods were then performed on the same system, in both cases starting with the initial connate water saturation. The floods were run with a superficial velocity of about 1/8 ft/D. Fig. 15 shows the oil recovery curves obtained from these two polymer floods. Prior to the first polymer flood, polymer had not contacted the sand so that adsorption can be presumed active during the flood. The second flood was performed using the same sand pack so that adsorption was minimal or absent. The slightly higher recovery in flood No. 2 probably reflects this lesser adsorption.

The sand pack had three pressure taps, one in the center and two 10-in. either side. The absolute permeability of the core (100 percent water saturated) was lowered by about 15 percent after Kelzan had contacted the sand. However, the measured relative permeability to water at residual oil was reduced by a factor of 3 after Kelzan had contacted the sand. This reduction was permanent in that it persisted after flushing with a large volume of normal water. The reduction in relative permeability to polymer water at residual oil was the same between Taps 1 and 2 and between Taps 2 and 3. That is, there was no indication of plugging near the inlet end of the sand pack. Pressure drop and flow rate measurements during flow of the 268-ppm Kelzan solution in a core containing no oil indicated an effective viscosity of 3 cp.

Contrary to expectation, analysis of the water produced in the polymer floods showed all but the first small increment to contain some polymer. The concentration did remain quite low (less than 15 percent of feed) until a volume of water equal to all the connate water plus about 0.12 PV had been produced. This appearance of polymer in the first water produced indicates a far less efficient displacement of the less viscous connate water than reported by Brown[9] in his experiments where injection water and connate water were of the same viscosity.

WATER INJECTED, PORE VOLUMES

FIG. 14 — INJECTION WATER DISPERSES POLYMER BANK.
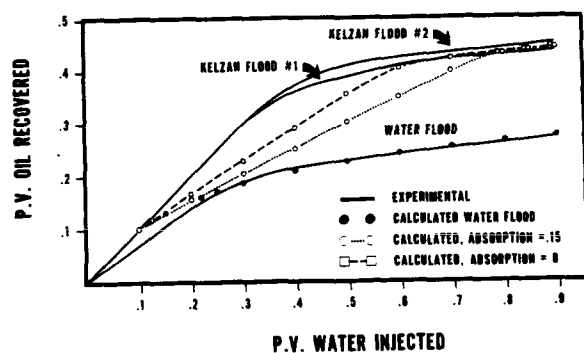

P.V. WATER INJECTED

FIG. 15 — EXPERIMENTAL AND CALCULATED OIL RECOVERY CURVES FOR LABORATORY WATER AND POLYMER FLOODS.

One possible explanation of this inefficient displacement of connate water by the injected polymer water is that it is simply a short-core effect. That is, it is caused by normal mixing or dispersion at the leading edge of the polymer front. If this is the case, then longer-core experiments should show a greater tendency toward production of a zero concentration connate water bank prior to polymer water breakthrough.

A second, and we believe more probable, explanation is that the hydrated polymer molecules are too large to pass some of the tight, connate water-saturated pores. These colloidal particles could physically block the smaller capillaries, thus making displacement of the connate water very difficult at best. The reduced relative permeability at residual oil to polymer water as compared to normal water gives some support to this argument. This explanation is essentially in agreement with the arguments of various authors[4,5,8] in support of their observed polymer solution mobilities which were lower than expected from viscosity measurements.

COMPARISON OF EXPERIMENTAL AND NUMERICAL MODEL RESULTS

The numerical model was run for the case of a single tube to simulate the linear waterflood and two polymer floods. The relative permeability curves shown in Fig. 2 are one of a number of sets measured for different mesh-size Nevada sands having permeabilities ranging down to 300 md. As stated above, these curves were provided by an oil company. No alterations of the 6,000-md curves were made to attempt to match the waterflood oil recovery curve. Fig. 15 shows that the waterflood oil recovery curve calculated by the numerical model agrees well with the experimental data. This indicates that the given relative permeability curves are closely representative of the true curves for the 6,000-md sand.

The circular and square points on Fig. 15 show the numerically calculated oil recovery curves for the two polymer floods with adsorption factor b = 0.15 and 0, respectively. A polymer water viscosity of 3 cp and polymer water relative permeability curve of 1/3, shown in Fig. 2, were used in the calculations. The linear portions of these two calculated recovery curves reflect the formation, high rate of travel, and production of the constant-saturation connate water bank (Fig. 4) ahead of the polymer front. Comparison with the experimental recovery curves shows that the numerical model predicts a considerably lower rate of production of the additional oil obtained by the polymer injection. The reason for this discrepancy is that the highly mobile connate water bank did not form in the experimental floods. The polymer water incompletely displaced and mixed with this connate water.

If the connate water bank failed to form in the experimental floods simply because of normal dispersion in the short core, then the numerically

calculated recovery curve should be more representative of a field-scale linear polymer flood. This follows from the fact that the mixed-zone length caused by dispersion in field-scale lengths will represent a much smaller percentage of distance traveled than in the laboratory-scale flood.

If the absence of the connate water bank in the laboratory floods reflects a polymer flood mechanism or characteristic independent of scale, then the oil recovery predicted by the numerical model is conservative.

PREDICTION OF FIELD-SCALE FIVE-SPOT POLYMER FLOOD

The numerical model was run to predict oil recovery from a five-spot polymer flood in a California viscous-oil reservoir. The relative permeability curves used corresponded to a 510-md Nevada sand representative of that reservoir. Oil viscosity was 34 cp, water viscosity 1 cp and polymer water viscosity was represented by $1 + 2C/C_0$. Feed concentration was 268-ppm Kelzan M and an adsorption level corresponding to $b = 0.15$ was used. The relative permeability curve for polymer water was taken as 1/3 the normal water relative permeability curve. Initial connate water saturation was 26.6 percent.

Fig. 16 shows the numerically calculated oil recovery for the three cases of 0.15, 0.3 and 0.5 PV polymer bank sizes. The numerically calculated five-spot waterflood recovery curve is shown for comparison. The calculated recoveries for the waterflood and the 0.3 PV bank polymer flood after injection of 1 PV are 0.257 and 0.366 PV oil, respectively. These figures give 0.109 bbl incremental oil from the polymer flood for 0.3 bbl of polymer water injected, or 0.363 bbl oil per bbl of polymer water. This represents about $8.35 incremental oil per $1.00 of polymer injected. This figure is based on $3/bbl of oil and a polymer cost of 13¢/bbl of 270-ppm Kelzan solution. In addition, the lower water-oil ratio during the polymer flood will reduce water handling costs.

The calculated recoveries for the waterflood and polymer flood after 0.5 PV injected are 0.21 and 0.27 PV oil, respectively. These recoveries yield
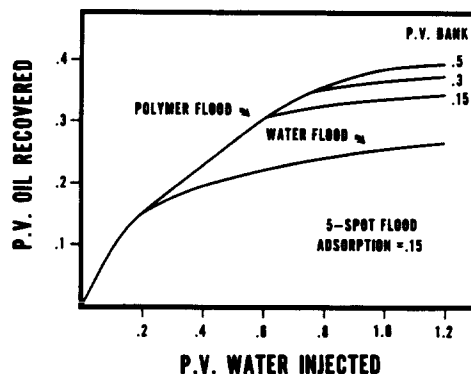

FIG. 16—CALCULATED OIL RECOVERY BY POLYMER SLUG INJECTION.

a figure of $4.60 incremental oil/$100 of polymer injected.

Fig. 17 shows the sensitivity of the predicted oil recovery from the polymer flood to the level of adsorption.

Fig. 18 shows calculated five-spot injectivities for the waterflood and polymer flood. While the waterflood injectivity increases more rapidly in early stages, the curves cross at 0.8 PV injected and the polymer flood injectivity is considerably higher after that point. The injectivity of 0.49 BPD/psi calculated by the model at the start of the floods agrees exactly with Eq. 6 using the properties

$$k = 510 \text{ md} \times 0.00633$$
$$\mu = 34 \text{ cp}$$
$$r_w = 14 \text{ in.}$$
$$h = 50 \text{ ft}$$
$$d = 330 \times \sqrt{2} \text{ ft}$$
$$\text{injectivity} = q/5.6146 \Delta p \text{ BPD/psi}$$

CONCLUSIONS

Results of this experimental and numerical study indicate the following:

1. Estimates of additional oil recovery by five-spot polymer flooding in a California viscous-oil reservoir are 0.2 and 0.363 bbl oil per bbl of 270-ppm Kelzan polymer solution after injection of 0.5 and 1 PV, respectively. These recoveries correspond respectively to $4.60 and $8.35 of additional oil per $1.00 of polymer injected.

2. Laboratory tests indicated that a 3-cp polymer solution exhibited a ninefold reduction in mobility at residual oil compared with normal water. This reduction in mobility, in excess of that expected from the viscosity effect alone, has been noted and reported by various authors using other polymers.[4,5,8]

3. Laboratory-oil displacement tests using 270-ppm Kelzan solutions showed that a connate water bank did not form in the 36-in. linear sand pack. That is, polymer was present in the first water produced.

4. An analytical method for solution of the linear polymer flood problem is presented. Complete displacement of the connate water by the injected polymer water is an assumption in this method. This easily used method gives a quick estimate of the additional oil recoverable by a line-drive polymer
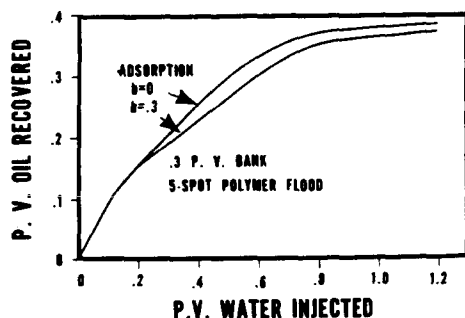
flood and provides a check on accuracy of numerical models for simulation of polymer flooding. Application in cases where the assumption of complete connate water displacement is not valid will yield a conservative estimate of the rate of recovery of the additional oil recoverable by polymer flooding.

5. A numerical model is presented for simulation of linear five-spot polymer flooding in single-layer or stratified reservoirs. The model accounts for effects of polymer slug size; adsorption (including losses by mechanical entrapment); relative permeability relationships; water viscosity dependence upon concentration and shear rate; reservoir heterogeneity through varying layer properties of permeability, porosity, thickness and relative permeability curves; initial level of water saturation (connate or mobile); and initial gas saturation. The model predicts the oil recovery curve, WOR and injectivity index as functions of pore volumes water injected. Checks against an analytical five-spot injectivity formula, the analytical linear polymer flood solution, and laboratory five-spot waterflood data indicate accuracy of the model. The model is based on the assumption of complete connate water displacement by the injected polymer water and will yield a conservative estimate of oil recovery rate from a polymer flood if that assumption is invalid.

NOMENCLATURE

A = cross-sectional area of tube

b = chord slope of adsorption isotherm at feed concentration (Fig. 1)

C = polymer concentration, mass/volume

C_s = adsorbed polymer concentration, mass/volume pore space

C_o = concentration of injected polymer water

D = dispersion coefficient, area/time

f = fractional flow of water, $\lambda_w/(\lambda_w + \lambda_o)$

I = pore volumes injected

k = absolute permeability

FIG. 17 — CALCULATED EFFECT OF ADSORPTION ON OIL RECOVERY.
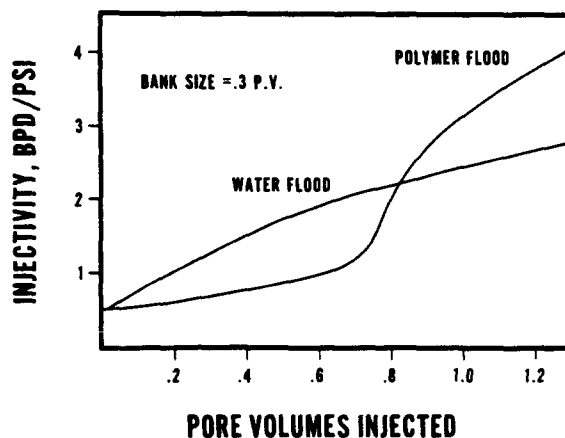

PORE VOLUMES INJECTED

FIG. 18 — CALCULATED FIVE-SPOT INJECTIVITY FOR WATERFLOOD AND POLYMER FLOOD.

k_r = relative permeability

L = length of linear system

S = water saturation

S_i = initial water saturation or S at Grid Point i

x_D = dimensionless distance

x = distance

t = time

u = volumetric velocity, vol/(area-time)

α = $\Delta l/\Delta x_D$

λ_w = water mobility, k_{rw}/μ_w

λ_o = oil mobility, k_{ro}/μ_o

λ = $\lambda_o + \lambda_w$

μ = viscosity

ϕ = porosity

SUBSCRIPTS

w = water

o = oil

REFERENCES

1. Detling, K. D.: "Process of Recovering Oil from Oil Sands", U.S. Patent 2,341,500 (Feb. 8, 1944).

2. Caudle, B. H. and Witte, M. D.: "Production Potential Changes During Sweep-Out in a Five-Spot System", *Trans.*, AIME (1959) Vol. 216, 446-448.

3. Gogarty, W. B.: "Mobility Control with Polymer Solutions", *Soc. Pet. Eng. J.* (June, 1967) 161-170.

4. Sandiford, B. B.: "Laboratory and Field Studies of Water Floods Using Polymer Solutions to Increase Oil Recoveries", *J. Pet. Tech.* (Aug., 1964) 917-922.

5. Pye, D. J.: "Improved Secondary Recovery by Control of Water Mobility", *J. Pet. Tech.* (Aug., 1964) 911-916.

6. Mungan, N., Smith, F. W. and Thompson, J. L.: "Some Aspects of Polymer Floods", *J. Pet. Tech.* (Sept., 1966) 1143-1150.

7. Jones, M. A.: "Waterflood Mobility Control: A Case History", *J. Pet. Tech.* (Sept., 1966) 1151-1156.

8. Dauben, D. L. and Menzie, D. E.: "The Flow of Polymer Solutions Through Porous Media", *J. Pet. Tech.* (Aug., 1967) 1065-1072.

9. Brown, W. O.: "Mobility of Connate Water During a Water Flood", *Trans.*, AIME (1957) Vol. 210, 190-195.

10. Buckley, S. E. and Leverett, M. C.: "Mechanism of Fluid Displacement in Sands", *Trans.*, AIME (1942) Vol. 146, 107-116.

11. Higgins, R. V. and Leighton, A. J.: "A Computer Method to Calculate Two-Phase Flow in Any Irregularly Bounded Porous Medium", *J. Pet. Tech.* (June, 1962) 679-683.

12. Muskat, M.: *The Flow of Homogeneous Fluids Through Porous Media*, J. W. Edwards Publishing Co., Ann Arbor, Mich. (1946).

13. Douglas, Jim, Jr., Peaceman, D. W. and Rachford, H. H., Jr.: "A Method for Calculating Multi-Dimensional Immiscible Displacement", *Trans.*, AIME (1959) Vol. 216, 297-306.

14. Perkins, T. K., Jr. and Johnson, O. C.: "A Review of Diffusion and Dispersion in Porous Media", *Soc. Pet. Eng. J.* (March, 1963) 70-84.

APPENDIX

NUMERICAL MODEL FOR SIMULATION OF FIVE-SPOT POLYMER FLOODS

Assumptions in this numerical model are:

A. No dispersion at the leading edge of the polymer slug.

B. Complete displacement of connate water by the injected polymer water.

C. Instantaneous and irreversible adsorption (including mechanical entrapment) of polymer.

D. Isothermal flow of incompressible water and oil.

E. Any initial mobile gas saturation is produced ahead of oil.

F. Negligible effects of water-oil capillary pressure.

Factors accounted for in the model are:

(a) dispersion of the trailing edge of the polymer slug,

(b) displacement efficiency and areal sweep efficiency,

(c) polymer adsorption, and

(d) layered heterogeneity of the reservoir — permeability, porosity, thickness, initial water and gas saturations, relative permeability curves, adsorption level can all vary among the layers.

Assumption A is a difficult one to either justify or negate. On the one hand, polymer adsorption according to the isotherm shape of Fig. 1 and the favorable viscosity ratio of polymer water to normal water act to produce a sharp polymer concentration front. On the other hand, the polymer water-normal water *mobility* ratio at the leading edge of the polymer slug (Fig. 4) may be unfavorable. If the "adsorption" is actually mostly or all mechanical entrapment, then the adsorption isotherm may not have the "front-sharpening" characteristic of negative curvature shown in Fig. 1. Assumptions A and B are to an extent related, since incomplete displacement of connate water by the polymer water will tend to dilute the polymer water at the displacement front with subsequent mixing or dispersion. We can say, however, that our laboratory oil recovery curves *indicate* that Assumptions A and B will yield a conservative *estimate* of the rate of oil recovery in cases where the assumptions are invalid.

We now proceed to describe the numerical model. One-eighth of a five-spot is divided into NT tubes; the tubes are defined by drawing straight lines from the injector and the producer to the perpendicular bisector of the right triangle representing the 1/8 five-spot. The angles between these lines are all equal. Higgins and Leighton[11] proposed use of the true streamtubes as determined from a potential flow calculation for a unit mobility ratio flood. We find insignificant difference in predictions using these simpler triangular tubes.

Elementary trigonometry gives cumulative volume and cross-sectional area A of each tube as functions of distance along its center line from the injector

to the producer. Darcy's law gives for any tube

$$q = -kA\lambda \frac{\partial p}{\partial x} \quad \ldots \ldots \ldots \ldots , \text{(A-1)}$$

where λ is total mobility, $\lambda_w + \lambda_o$. Integration of this equation from injector to producer (x_I to x_L) gives

$$\frac{q}{k\Delta p} = 1/\int_{x_1}^{x_L} \frac{dx}{A(x)\lambda(S)} \quad \ldots \ldots \text{(A-2)}$$

We divide the tube into N equal-volume increments, denote them by index $i = 1, 2,\ldots,N$, and approximate the integral as

$$\int_{x_1}^{x_L} \frac{dx}{A(x)\lambda(S)} \cong \sum_{i=1}^{N} \frac{1}{\lambda_i} \int_{x_{i-\frac{1}{2}}}^{x_{i+\frac{1}{2}}} \frac{dx}{A(x)}$$

$$\ldots \ldots \text{(A-3)}$$

Since cross-sectional area A is a linear function of x within a given block, this gives

$$\int_{x_1}^{x_L} \frac{dx}{A(x)\lambda(S)} \cong$$

$$\sum_{i=1}^{N} \frac{\Delta x_i}{\lambda_i} \frac{\ln(A_{i+\frac{1}{2}}/A_{i-\frac{1}{2}})}{A_{i+\frac{1}{2}} - A_{i-\frac{1}{2}}} \quad . \text{(A-4)}$$

The term λ_i is the value of total mobility evaluated at $S=S_i$ and $C=C_i$. We denote the tubes by index $j=1, 2,\ldots, NT$. From Eqs. A-3 and A-4 the flow rate q_j through tube j is given by

$$q_j = K_j \Delta p \cdot \ldots \ldots \ldots \ldots \ldots \text{(A-5)}$$

where Δp is pressure drop from injector to producer, the same for all tubes, and

$$K_j = \left[k_j\right] \Big/ \left[\sum_{i=1}^{N} \frac{\Delta x_i}{\lambda_i}\right.$$

$$\left. \ln(A_{i+\frac{1}{2}}/A_{i-\frac{1}{2}})/(A_{i+\frac{1}{2}} - A_{i-\frac{1}{2}})\right]$$

$$\ldots \ldots \ldots \ldots \ldots \ldots \text{(A-6)}$$

For each time step, the injection rate into tube j is then calculated as

$$q_j = \frac{K_j}{\sum_{j=1}^{NT} K_j} q \quad , \ldots \ldots \ldots \text{(A-7)}$$

where q is 1/8 the total injection rate into the

the injector. The injectivity index for the entire five-spot is simply $8 \sum_{j=1}^{NT} K_j$.

For water-oil flow in a tube of varying cross-sectional area, the mass conservation Eq. 1 are

$$-q \frac{\partial f}{\partial x} = \phi A \frac{\partial S}{\partial t} \quad \ldots \ldots \ldots \text{(A-8a)}$$

$$-q \frac{\partial fC}{\partial x} = \phi A \left[\frac{\partial SC}{\partial t} + \frac{\partial C_s}{\partial t}\right], \ldots \text{(A-8b)}$$

where q is total volumetric flow rate, a constant independent of distance along the tube. Constancy of q is a consequence of the assumption of fluid and rock incompressibility. Defining the new variables of dimensionless distance (x_D) and pore volumes injected (I)

$$x_D = \phi \int_{x_1}^{x} A(x)\, dx/V_t$$

$$I = qt/V_t \qquad \ldots \ldots \text{(A-9)}$$

we find that Eqs. A-8a and A-8b

$$-\frac{\partial f}{\partial x_D} = \frac{\partial S}{\partial I} \quad \ldots \ldots \ldots \ldots \text{(A-10a)}$$

$$-\frac{\partial fC}{\partial x_D} = \frac{\partial SC}{\partial I} + \frac{\partial C_s}{\partial I} \quad \ldots \ldots \text{(A-10b)}$$

The term V_T is total tube pore volume.

Eqs. A-10a and A-10b are replaced by the finite-difference approximations

$$\frac{f_{i-1,n+\frac{1}{2}} - f_{i,n+\frac{1}{2}}}{\Delta x_D} =$$

$$\frac{S_{i,n+1} - S_{i,n}}{\Delta I} \quad \ldots \ldots \text{(A-11a)}$$

$$\frac{f_{i-1,n+\frac{1}{2}}C_{i-1,n} - f_{i,n+\frac{1}{2}}C_{i,n}}{\Delta x_D} =$$

$$\frac{(SC)_{i,n+1} - (SC)_{i,n}}{\Delta I} +$$

$$\frac{C_{si,n+1} - C_{si,n}}{\Delta I} \quad \ldots \ldots \text{(A-11b)}$$

where index i denotes the grid blocks and n denotes time, i.e., $C_{i,n}$ is the value of C in the i grid block at time $I = I_n$. Eq. A-11a is solved first using the

old concentration values $C_{i,n}$ to evaluate water viscosity in the fractional flow terms. For C fixed at C_n we have

$$f_{i,n+\frac{1}{2}} = f_{i,n} + .5f_i'(S_{i,n+1} - S_{i,n}) \quad \ldots \ldots (A\text{-}12)$$

where f_i' is $(\partial f/\partial S)$. Inserting Eq. A-12 into Eq. A-11a and rearrangement gives

$$S_{i,n+1} = [S_{i,n}(1 + .5f_i'\alpha) + \alpha(f_{i-1,n+\frac{1}{2}} - f_{i,n})]/ (1 + .5\alpha f_i') \quad \ldots \ldots (A\text{-}13)$$

where α is $\Delta l/\Delta x_D$ and $f_{i-1,n+\frac{1}{2}}$ is known since calculations of $S_{i,n+1}$ are performed from left to right, $i = 1, 2, 3, \ldots, N$. The term f' is iterated to the value $(f_{i,n+1}-f_{i,n})/(S_{i,n+1}-S_{i,n})$. The difference representation (Eq. A-11a) is unconditionally stable. Truncation error of the explicit form with n rather than $n+\frac{1}{2}$ on the left-hand side of Eq. A-11a is less than that of Eq. A-11a, but the stability condition $\Delta l \leq \Delta x_D/f'$ results.

After solution of Eq. A-11a for $S_{i,n+1}$ (and $f_{i,n+\frac{1}{2}}$) at all i, the concentration Eq. A-11b is solved. The explicit form of this equation is used to take advantage of the considerably lower truncation error compared with that of the implicit form. This truncation error contributes the numerical dispersion so often dominant in numerical attempts to solve equations of type Eq. A-10b. At the trailing edge of the polymer slug where we are concerned with dispersion, the adsorption term is zero (Assumption C) and Eq. A-11b gives

$$S_{i,n+1}C_{i,n+1} = S_{i,n}C_{i,n} + \alpha[f_{i-1,n+\frac{1}{2}} \cdot C_{i-1,n} - f_{i,n+\frac{1}{2}}C_{i,n}] \quad \ldots \ldots \ldots (A\text{-}14)$$

Numerical dispersion is eliminated entirely in solution of Eq. A-14 if the value of α is chosen as

$$\alpha = S_{i,n}/f_{i,n+\frac{1}{2}} , \quad \ldots \ldots (A\text{-}15)$$

in which case Eq. A-14 becomes

$$C_{i,n+1} = \alpha f_{i-1,n+\frac{1}{2}}C_{i-1,n}/S_{i,n+1}$$

$$\ldots \ldots \ldots \ldots \ldots (A\text{-}16)$$

Eq. A-16 preserves an exactly sharp trailing edge of the slug which is the true solution for the case of zero dispersion. This elimination of numerical dispersion is actually, of course, simply an elimination of truncation error. The truncation error in Eq. A-11a causing the numerical dispersion is a difference of two positive terms while in the implicit difference approximation to Eq. A-10b the truncation error is a sum of two positive terms. Selection of distance and time increments according to Eq. A-15 results in exact cancellation of these truncation error terms in the explicit difference approximation.

The case of nonzero dispersion at the trailing edge is simulated by simply using α values less than given by Eq. A-15. The particular values used for Δx_D and Δl can be quantitatively related to the effective value of the dispersion coefficient D. This relationship will be shown here for the somewhat simpler equation

$$D\frac{\partial^2 C}{\partial x^2} - u\frac{\partial C}{\partial x} = \phi\frac{\partial C}{\partial t} \quad \ldots \ldots (A\text{-}17)$$

Defining $l = ut/L\phi$ and $x_D = x/L$, and replacing $\partial C/\partial x_D$ and $\partial C/\partial l$ by finite difference forms from Taylor's series gives

$$\frac{D}{Lu} C_{xx} + \frac{1}{2}(\Delta l - \Delta x_D) C_{xx} + \frac{\Delta l}{2} \frac{D}{Lu} (\frac{D}{Lu} C_{xxxx} - 2C_{xxx}) - \frac{C_{i,n} - C_{i-1,n}}{\Delta x_D} = \frac{C_{i,n+1} - C_{i,n}}{\Delta l}$$

$$\ldots \ldots \ldots (A\text{-}18)$$

where C_{xx} is $\partial^2 C/\partial x_D^2$. Because of the normal values of D/Lu (less than 1) and the lower values of higher spatial derivatives, the value of $\frac{D\Delta l}{2Lu}\left(\frac{D}{Lu}C_{xxxx} - 2C_{xxx}\right)$ can be ignored as a first and good approximation. We then have that explicit difference equation

$$- \frac{C_{i,n} - C_{i-1,n}}{\Delta x_D} = \frac{C_{i,n+1} - C_{i,n}}{\Delta l}$$

$$\ldots \ldots \ldots \ldots \ldots \ldots (A\text{-}19)$$

is actually a difference approximation to the Eq. A-17, including dispersion for the case where

$$\frac{D}{Lu} = \frac{1}{2}(\Delta x_D - \Delta l). \quad \ldots \ldots (A\text{-}20)$$

As noted above in discussion of Eqs. A-14 through A-16, if Δx_D is set equal to Δl, we obtain an exact solution to the equation $-u\partial C/\partial x = \phi\partial C/\partial t$ with

zero numerical dispersion. Actual comparison of solutions to Eq. A-19 using $\Delta l < \Delta x_D$ with analytical solutions to Eq. A-17 using D values from Eq. A-20 showed very good agreement.

In a somewhat laborious fashion it can be shown that Eq. A-14 using

$$\alpha = (1 - \underline{D})S_{i,n}/f_{i,n+\frac{1}{2}} \qquad . \quad . \text{(A-21)}$$

results in a solution of Eq. A-10b with a dispersion term $D\partial^2 C/\partial x^2$ present on the left-hand side and a quantitative relationship between the value of D and the true dispersion coefficient D. The "dispersion" of 0.3 and 0.7 mentioned earlier in the paper in connection with Figs. 10 and 11 refers to the value of D in Eq. A-21. An extrapolation procedure is used to estimate $f_{i,n+\frac{1}{2}}$ in order to calculate α from Eq. A-21 at the start of the time step.

Boundary conditions for solution of Eqs. A-13 and A-14 are

$$
\begin{aligned}
f_{o,n} &= 1.0 \\
c_{o,n} &= g_n \quad , \qquad . \quad . \quad . \quad . \quad . \quad . \quad . \quad . \quad \text{(A-22)}
\end{aligned}
$$

where g_n is a specified function of time n. For a slug injection g_n is feed concentration for $0 < n < n_1$ and 0 otherwise where l_{n_1} is the slug size. For a polymer flood initiated at some stage during a waterflood, g_n is feed concentration for $n_1 < n < n_2$ and 0 otherwise where l_{n_1} is the time at the start of polymer injection and $l_{n_1} - l_{n_2}$ slug size.

★ ★ ★